ISSN: 1410-8917
e-ISSN: 2597-9914

Jurnal Kimia Sains dan Aplikasi 29 (1) (2026): 30-38

Jurnal Kimia Sains dan Aplikasi
Journal of Scientific and Applied Chemistry

Journal homepage: http://ejournal.undip.ac.id/index.php/ksa

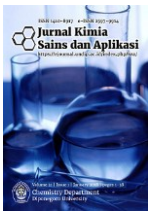

In Silico Study of Organo-selenium with PPAR-γ and NF-κB Receptors for Cardiovascular Protection

Ayu Shalihat [1,*], Cecep Suhandi [2], Aliya Nur Hasanah [1], Mutakin [1]

[1] Department of Pharmaceutical Analysis and Medicinal Chemistry, Faculty of Pharmacy, Universitas Padjadjaran, Sumedang, Indonesia
[2] Department of Pharmaceutics and Technological Pharmacy, Faculty of Pharmacy, Universitas Padjadjaran, Sumedang, Indonesia

* Corresponding author: ayu.shalihat@unpad.ac.id

https://doi.org/10.14710/jksa.29.1.30-38

Article Info

Article history:

Received: 21st October 2025
Revised: 06th January 2026
Accepted: 07th January 2026
Online: 07th February 2026

Keywords:
Cardio-protection; molecular docking; molecular dynamic; organo-selenium; PPAR-γ; NF- κB

Abstract

Cardiovascular disease (CVD) continues to represent a significant global health challenge, leading to the need for new and more effective therapeutic approaches. Organo-selenium compounds have potential as antioxidants and anti-inflammatory agents, which may help protect the heart and vascular system. However, the molecular mechanisms by which Organo-selenium exerts its cardioprotective effects are still not fully understood. The interaction with key regulatory pathways such as peroxisome proliferator-activated receptor gamma (PPAR-γ) and nuclear factor kappa B (NF-κB) has not been clearly defined. Therefore, this study aims to investigate the molecular interactions between organo-selenium compounds and the PPAR-γ and NF-κB-inducing kinase receptors in the context of cardiovascular protection. Molecular docking simulations were performed using the ligand-binding domain of PPAR-γ and the 20 organo-selenium ligands. The binding affinities and interactions between organo-selenium and receptors were analyzed. Among the screened organo-selenium ligands, compound 13 exhibited the most favorable binding affinity toward both PPAR-γ and NF-κB compared to the native ligand. Based on these results, compound 13 was selected for molecular dynamics simulations. The molecular dynamics study, using parameters such as RMSD, RMSF, SASA, and the Gyration plot, shows that compound 13 with PPAR-γ exhibits better stability and flexibility. At the same time, the NF-κB interaction, though stable, may be less energetically favorable than the native ligand. These interactions suggest that compound 13 (Ebselen) may modulate PPAR-γ activity, thereby influencing cell signaling pathways involved in cardiac protection. Overall, the findings suggest that modulation of the PPAR-γ pathway by compound 13 may represent a promising mechanism in cell signaling for cardiovascular protection.

1. Introduction

Cardiovascular disease remains the leading cause of death worldwide [1]. Various risk factors can contribute to the development of heart disease, such as smoking, lack of physical activity, dietary intake, and other conditions like hypertension and diabetes [2]. One essential nutrient for heart cells is selenium, and its deficiency can lead to cell damage and conditions like Keshan disease [3, 4]. Previous research has shown that selenium provides cardioprotective effects by inhibiting necrosis [5], reducing apoptosis and autophagy [6], and decreasing inflammation [7].

Ongoing research is continuously developing cardioprotective studies, encompassing in vitro and in vivo approaches, as well as in silico investigations. These developments aim to understand the mechanisms of cardiac protection, treatment strategies that activate heart cell signaling pathways, and novel cardioprotective therapies [8]. In vitro and in vivo studies have demonstrated the cardioprotective effects of selenium through molecular mechanisms in cell signalling

pathways, including its ability to reduce apoptosis and autophagy, induced via the peroxisome proliferator-activated receptor (PPAR-γ) pathway [9]. PPAR-γ plays a crucial role in maintaining energy homeostasis [10] and functions as a ligand-induced transcription factor that inhibits inflammatory responses in cardiac tissue, thereby minimizing pathological damage in ischemic heart conditions [11].

Selenium has been reported to contribute to cellular protection by modulating the NF-κB signaling pathway, which regulates proinflammatory cytokine expression. Since NF-κB activation is associated with inflammation-induced cardiomyocyte apoptosis and functional impairment, molecular interactions with this pathway are commonly interpreted in the context of pathway attenuation to support cellular protection [12]. PPAR-γ and NF-κB are distinct signaling pathways; however, they exhibit functional crosstalk [13], in which PPAR-γ activation negatively regulates NF-κB signaling, thereby contributing to the maintenance of redox homeostasis and the attenuation of oxidative stress and inflammation [14].

Organo-selenium compounds have been investigated for their potential cardioprotective effects [15]. Although several mechanisms have been studied, further research is needed to fully understand the organo-selenium mechanism in the PPAR-γ and NF-κB-inducing kinase pathway. Conducting in silico studies and predicting the binding of organo-selenium compounds to the protein receptor can provide insights into the mechanism of organo-selenium's cardioprotective effects on cell survival.

2. Experimental

2.1. Preparation of Ligand Structures

The 20 ligands were converted into two-dimensional (2D) structures and then into three-dimensional (3D) structures using ChemDraw 8.0 [16].

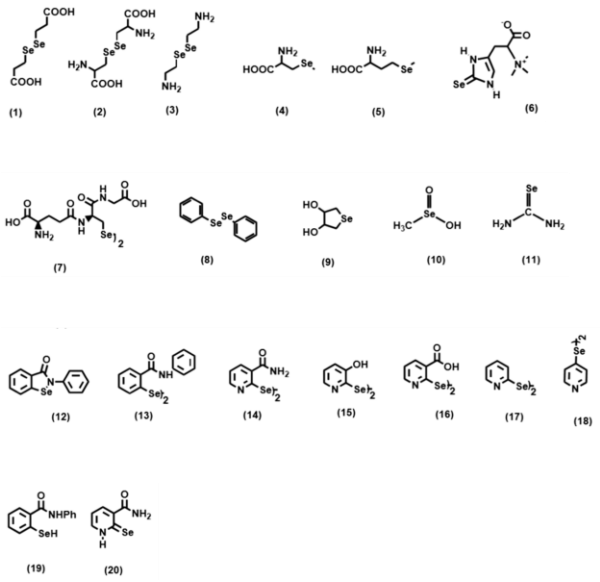

Figure 1. 2D structures of organo-selenium test ligands

2.2. Preparation of Receptors

High-resolution crystal structures of the ligand-binding domains of PPAR-γ complexed with rosiglitazone (PDB ID: 2PRG) and nuclear factor kappa B (NF-κB) inducing kinase, an upstream regulatory kinase involved in the non-canonical NF-κB signaling pathway. (PDB ID: 4IDV) were obtained from the Protein Data Bank with 4-{3-[2-amino-5-(2-methoxyethoxy)pyrimidin-4-yl]-1H-indol-5-yl}-2-methylbut-3-yn-2-ol as native ligand. The 3D structures were saved in PDB format, and all co-crystallized ligands, native ligands, and solvent molecules were removed before docking preparation. Hydrogen atoms were added to the protein structures, and the structures were then energy-minimized to optimize their geometry. Receptor and ligand preparations, including grid box determination for docking space and coordinate settings, were performed using AutoDock Tools version 1.5.6 [17, 18].

2.3. Validation of the Molecular Docking Method

Validation of the molecular docking protocol was performed using AutoDock Tools version 1.5.6 by re-docking the native ligand into the binding site of its corresponding target protein after removal of the original ligand. Water molecules within the receptor structure were removed, and the grid box was positioned using the native ligand coordinates before re-docking. The process was carried out to determine the root-mean-square deviation (RMSD); natural ligand redocking is considered successful if the RMSD is < 2 Å [19]. An RMSD value was obtained by looking at the overlay of the native ligand, which was separated before docking, and the redocked native ligand using Discovery Studio Visualizer.

2.4. Molecular Docking Simulation

The three-dimensional structures of the native and organo-selenium ligands were optimized using Chem3D Ultra 8.0, employing the MM2 semi-empirical method. Geometry optimization was performed to obtain the lowest energy conformation of each ligand. Molecular docking was then conducted by binding each ligand to its respective receptor in pdbqt format. The grid box coordinates were set at (x = 59.42, y = -5.61, z = 42.41) for PPAR-γ and (x = 16.11, y = 13.92, z = 87.36) for NF-κB (PDB ID: 4IDV), specifically the kinase active site (ATP-binding pocket), as defined by the co-crystallized native ligand [20], with a total of 50 docking poses generated for each complex. All ligands were treated as flexible, while receptor macromolecules were kept rigid during docking. The resulting binding energies and key molecular interactions, such as hydrogen bonding, hydrophobic interactions, and bond distances, were analyzed and visualized using Discovery Studio Visualizer.

2.5. Molecular Dynamics Simulation

Molecular dynamics simulations were performed on the organo-selenium compound with the lowest binding energy to the PPAR-γ receptor, as determined by molecular docking. The simulations were conducted with GROMACS 2016.3 using the AMBER99SB-ILDN force field [21]. Ligand topology and parameter files were generated using ACPYPE [22]. Long-range electrostatic interactions

were calculated using the particle mesh Ewald (PME) method [23], and the system was neutralized by adding Na^+ and Cl^- counterions. The complex was solvated in a cubic box using the TIP3P water model. Before the production phase, the system underwent energy minimization, followed by gradual heating to 310 K and equilibration under constant temperature and pressure. Subsequently, a 100-ns production run was performed using a 2-femtosecond timestep. Post-simulation analyses included calculations of the root-mean-square deviation (RMSD), root-mean-square fluctuation (RMSF), radius of gyration (Rg), and solvent-accessible surface area (SASA) to assess conformational stability and dominant molecular motions. Furthermore, the binding free energy of the protein–ligand complex was estimated using the Molecular Mechanics Poisson–Boltzmann Surface Area (MM-PBSA) method to provide a more accurate understanding of the interaction energetics [24].

3. Results and Discussion

3.1. Molecular Docking Validation and Simulations

The molecular docking of organo-selenium compounds with the PPAR-γ receptor yielded a validation score of 1.91, which meets the criterion (< 2 Å). Out of the 20 compounds tested, compound 13 exhibited a lower free energy compared to its natural ligand. The results of 20 organo-selenium compounds are presented in Table 1. These findings show that compound 13 has the lowest binding energy for the PPAR-γ receptor and may modulate its activity. The 2D and 3D visualizations of interactions are shown in Figure 2. PPAR-γ plays a vital role in preserving energy balance. Ligands activate this transcription factor and exert its effects by suppressing inflammatory responses in cardiac tissue, reducing ischemic damage to the heart [10, 11]. The test ligand was docked with PPAR-γ and showed that compound 13 had the lowest free binding energy (-10.79) compared to the native ligand (-9.37). The same interaction is observed in the amino acid residues Leu353, Leu469, Tyr327, Tyr473, Gln286, His323, His449, Met364, Gly284, and Arg288, predominantly through hydrophobic interactions with key residues that form the canonical ligand-binding pocket of PPAR-γ. This hydrophobic cavity is a defining structural feature of PPAR-γ and plays a role in stabilizing ligand orientation and the receptor–ligand complex [25].

The molecular docking of organo-selenium compounds with the NF-κB-inducing kinase receptor yielded a validation score of 1.732 Å, which meets the criterion of being lower than 2 Å. Of the 20 compounds tested, compound 13 had a lower free energy of -11.53 kcal/mol than its native ligand, -9.71 kcal/mol; the same interaction was observed in amino acid residues Gly409, Asp534, and Ser476. Although the interaction involved only a limited number of amino acid residues, the complex exhibited a more favorable binding free energy, suggesting that the formed interactions were well-positioned within the NF-κB-inducing kinase binding pocket. The results of 20 organo-selenium molecular docking with NF-κB are presented in Table 2. The 2D and 3D visualizations of the interactions between NF-κB and compound 13 are shown in Figure 3.

3.2. Molecular Dynamics

The ligand–receptor complexes of PPAR-γ and compound 13 were analyzed using molecular dynamics simulations over a 100-ns trajectory with GROMACS 2016. System stability throughout the 100-ns simulation was evaluated using RMSD and RMSF. Additionally, SASA and Rg were analyzed to assess solvent exposure and structural compactness, respectively [26]. The molecular dynamics trajectories of both complexes are depicted in Figures 4 and 5.

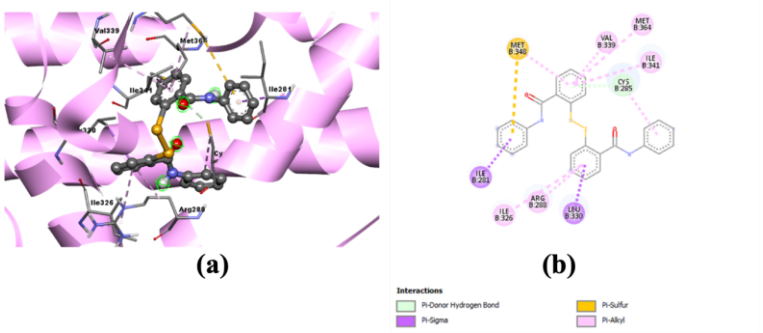

Figure 2. Visualization of the interaction of compound 13 and PPAR-γ receptor (a) 3D and (b) 2D

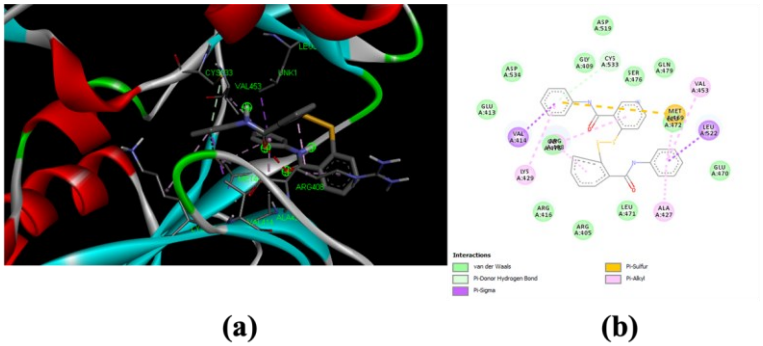

Figure 3. Visualization of the interaction of compound 13 and NF-κB receptor (a) 3D and (b) 2D

Table 1. Organo-selenium and PPAR-γ molecular docking results

Compound	Binding energy (kcal/mol)	Constant inhibition (μM)	Interaction	
			H-bond	Others
Native ligand	-9.37	0.13433	Cys285, Ser289, His323	Phe282, Phe363, Gly284, Tyr327, Tyr473, Lys367, Leu330, Leu453, Leu465, Leu469, Gln286, His323, His449, Ile326, Ala292, Arg288, Met364
1	-4.34	654.56	Tyr327, Lys367, Phe282, His449	Met364, Phe363, Ile362, Ser289, Leu330, Leu453, Leu469, Cys285, His323, Tyr473, Gln286
2	-4.02	1130	Cys285	Gly284, Ser342, Met348, Met364, Ile281, Ile341, Val339, Leu330, Leu333, Leu340, Leu353, Arg288
3	-4.23	796.15	Cys285, Ser289, Tyr473	Leu453, Leu469, Gln286, His323, His449, Phe282, Phe363, Ile326, Tyr327, Arg288
4	-3.62	2240	Tyr473	Cys285, Phe282, Phe363, His323, His449, Ser289, Tyr327, Leu453, Leu465, Leu469, Gln286
5	-3.99	1180	Tyr327, Lys367, Met364	Leu330, Leu 469, Gln286, Phe282, Phe363, Ser289, His323, His449, Cys285
6	-5.13	174.55	Tyr473, His449, Met364	Arg288, Ser289, Phe282, Phe363, Lys367, Gln286, Tyr327, Leu330, Leu469, Leu453, His323, Ile326, Cys285
7	-2.12	27890	Tyr327, Ile326, Arg280, Ser342	Met329, Met332, Met348, Met364, Lys367, Ile249, Ile281, Ile341, Phe363, Leu255, Leu330, Leu333, Leu340, Gly284, Val339, Cys285, Ala292, Ser289, Arg288
8	-7.08	6.48	-	Lys367, Phe363, Met364, Cys285, Leu330, Leu469, Arg288, Tyr327, Tyr473, His323, His449, Gln286, Ser289, Ile326
9	-5.34	122.07	Tyr473, His449	Tyr327, Phe363, His323, Ser289, Gln286, Leu453, Leu469, Cys285
10	-4.02	1140	Tyr473, Ser289	Leu453, Leu465, Leu469, His323, His449, Gln286, Cys285
11	-2.31	20260	Tyr473	Leu453, Leu465, Leu469, His323, His449, Gln286, Cys285, Tyr327, Ser289
12	-8.17	1.03	Ser289	Phe282, Phe363, Gln286, Leu330, Leu453, Leu465, Leu469, Tyr327, Tyr473, His323, His449, Ile326, Met364, Arg288, Cys285
13	-10.79	0.01238	-	Leu255, Leu330, Leu353, Leu469, Ile281, Ile326, Ile341, Met348, Met364, Gly284, Arg280, Arg288, Ser289, Ser342, Tyr327, Tyr473, His323, His449, Gln286, Cys285, Val339, Phe363
14	-8.15	1.07	Cys285, Tyr327, Met364, Lys367	Gln286, Ser289, Arg288, Ile326, Leu330, Leu333, Val339, Leu340, Ile341, Phe363, His449
15	-7.01	7.24	Tyr327, Met364	Leu330, Leu453, Leu465, Leu469, Phe282, Phe363, His323, His449, Ile326, Arg288, Cys285, Ser289, Lys367, Gln286, Tyr473
16	-7.35	4.11	His323, Tyr327, Lys367	Met364, Phe282, Phe363, Ile326, Leu330, Leu453, Leu465, Leu469, His449, Cys285, Ser289, Arg288, Gln286, Tyr473
17	-6.9	8.77	Cys285, Ser289, Tyr327, Tyr473	Leu330, Leu453, Leu465, Leu469, Phe282, Phe363, His323, His449, Ile326, Arg288, Gln286,
18	-5.99	40.7	Tyr473	Leu330, Leu453, Leu469, His323, His449, Ile326, Gln286, Arg288, Met329, Ala292, Cys285, Tyr327, Ser289,
19	-7.78	1.99	Phe282	Leu330, Leu469, Phe363, His323, His449, Lys367, Tyr327, Tyr473, Ile326, Gln286, Cys285, Arg288, Ser289
20	-5.51	91.41	Phe282, Ser289, Tyr473	Leu453, Leu465, Leu469, His323, His449, Ile281, Phe363, Cys285, Gln286

Table 2. Organo-selenium and NF-κB molecular docking results

Compound	Binding energy (kcal/mol)	Constant inhibition (μM)	Interaction	
			H-bond	Others
Native ligand	-9.71	0.07623	Glu440, Glu470	Phe535, Lys429, Cys444, Ile467, Leu522, Val414, Cys533, Leu472, Pro454, Val453, Ala427, Leu471, Gly536, Gly475, Gly409, Asp534, Arg408, Ser476
1	-5.86	50.88	Glu470, Arg408, Arg416, Leu406	Val453, Leu522, Met469, Val414, His415, Gly407, Arg405, Ala427, Leu472
2	-5.48	95.94	Asp519, Glu470	Asp534, Ser476, Asn 520, Gly409, Met469, Arg408, Ala427, Leu471, Val453, Leu472
3	-6.68	12.71	Glu413, Asp534, Asn520, Ser410	Leu522, Met469
4	-4.98	224.22	Arg416, Arg408, Leu406, Val414	Leu472, Arg405, Gly407, His415
5	-4.86	275.32	Leu406, Arg408, Arg416	Gly407, His415, Arg405, Val414, Leu472
6	-4.56	454.83	Asp519, Gly409	Gly475, Arg408, Leu522, Cys533, Ser410
7	-0.15	776390	Asp519, Gly409, Asp534, Ser476, Asn520, Glu470, Glu440	Lys517, Gln479, Arg 408, Cys 533, Leu522, Gly475, Ala427, Leu471, Val453, Ile467, Val414, Met469, Lys429, Glu413, Ser410
8	-6.88	9.01	-	Ser410, Asn520, Lys429, Glu440, Ile467, Leu455
9	-4.97	228.47	Glu440	Gly536, Lys429, Asp534, Ile467, Leu455
10	-3.79	1660	Asp534, Phe535, Met469	Cys533, Gly536, Lys429, Leu455, Ile 467, Cys 444, Val 453
11	-2.78	9230	Asn520, Asp519, Ser410	Leu522, Cys533, Gly409
12	-6.78	10.79	-	Gly409, Ser410, Glu413, Asp534, Val453, Glu470, Leu472, Leu471, Arg408
13	-11.53	0.00352	-	Asp519, Gly409, Ser476, Gln479, Asp534, Glu413
14	-7.54	2.96	Asp519, Leu472, Glu413	Arg408, Gly475, Leu471, Glu470, Ala427, Leu522, Met467, Val414, Cys533, Lys429, Asp534, Gly409, Ser410, Asn520, Ser476
15	-6.71	12.07	Leu472, Arg408, Leu406	Glu473, Arg405, His415, Leu471, Gly475
16	-7.32	4.28	Gln479, Arg408, Arg416, Leu406	Gly475, Val414, Ala427, Leu471, His415, Gly407, Leu522, Arg405, Gly409
17	-6.23	27.35	Leu472	Gly475, Leu471, His415, Arg405
18	-6.28	24.94	Glu470, Leu406	His415, Gly407, Pro454, Leu472
19	-7.12	6.03	Glu470, Leu472	His415, Leu406, Arg405, Val453
20	-5.30	130.21	Asp534, Asn520, Asp519, Ser410, Gly409	Gln479, Arg408, Val414, Leu522, Cys533

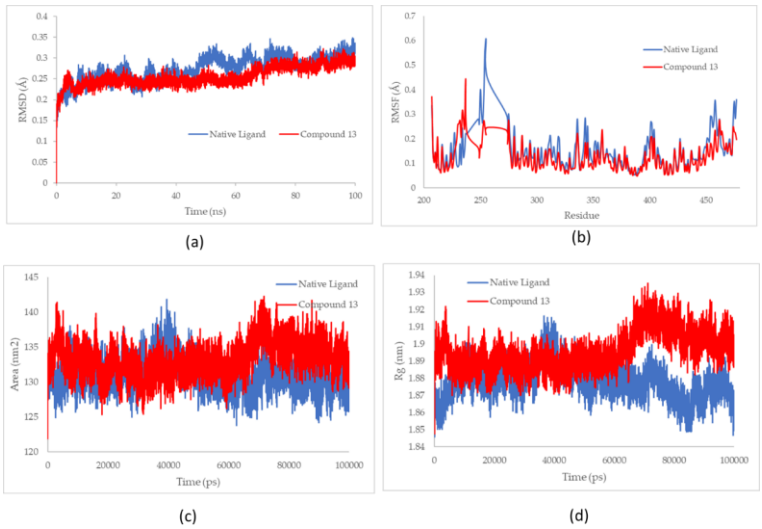

Figure 4. Molecular dynamics parameters of compound 13 and PPAR-γ: (a) RMSD, (b) RMSF, (c) SASA, and (d) Rg plot

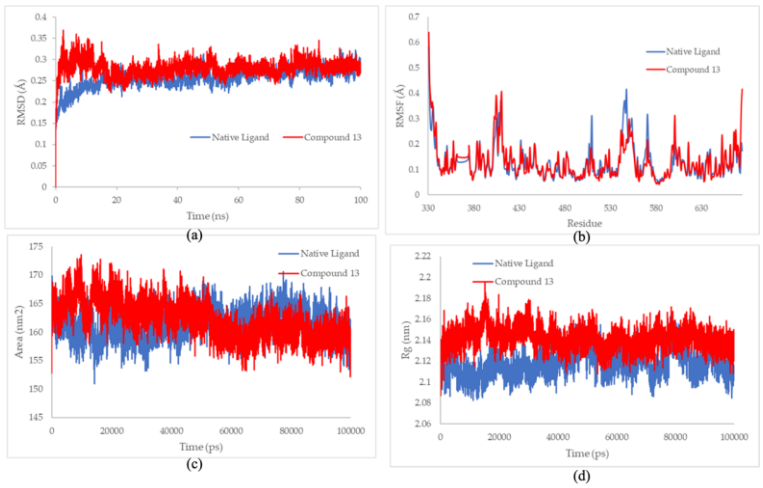

Figure 5. Molecular dynamic parameters of compound 13 and NF-κB inducing kinase (a) RMSD, (b) RMSF, (c) SASA, and (d) Rg plot

Molecular dynamics simulations were performed for both the native ligand complex and the compound 13 complex. RMSD analysis was employed to assess structural stability and conformational changes throughout the simulation. The organo-selenium complex exhibited lower RMSD fluctuations than the native ligand, indicating a more stable and consistent binding conformation of compound 13 within the PPAR-γ active site. RMSF analysis showed similar flexibility profiles across amino acid residues for both complexes, implying that the binding of compound 13 does not induce significant conformational disturbances in the receptor.

The SASA profile indicated that the native ligand–PPAR-γ complex exhibited lower surface area fluctuations than compound 13, suggesting a compact binding mode. This contrasted with the RMSD results, which indicated conformational stability for compound 13. The Rg plots of complexes displayed comparable profiles, with Rg values of 1.87 nm (for the native ligand) and 1.89 nm (for compound 13), signifying minimal variation in global compactness the simulation. PPAR-γ activation is associated with cardioprotective effects through adiponectin regulation and modulation of inflammatory and oxidative stress pathways involved in cardiomyocyte survival, as well as regulation of glucose metabolism, insulin sensitivity, and adipokine expression, linking its activation to metabolic disorders such as diabetes and obesity that are associated with cardiovascular risk [27]. Although PPAR-γ activation is associated with cardioprotective effects, its pharmacological activation has been linked to adverse outcomes, weight gain, and fluid retention, suggesting that PPAR-γ agonists require careful, context-dependent evaluation and monitoring [28].

The NF-κB-inducing kinase–ligand complexes in molecular dynamics analysis showed distinct interaction behavior. The RMSD plot demonstrated that the native ligand maintained slightly lower deviations during the simulation, implying greater overall stability compared to compound 13. Nevertheless, compound 13 achieved equilibrium after approximately 30 ns and remained stable thereafter, indicating good adaptability within the NF-κB binding pocket. RMSF analysis revealed minor fluctuations in loop regions; however, overall, both complexes displayed similar residue-level flexibility patterns, suggesting that compound 13 binding does not induce large conformational rearrangements in NF-κB-inducing kinase.

Table 3. MM-PBSA energy summary of ligand–receptors during the 100-ns simulation

Receptors	Ligand	van der Waals energy (kJ/mol)	Electrostatic energy (kJ/mol)	Polar solvation energy (kJ/mol)	SASA energy (kJ/mol)	Total binding energy (kJ/mol)
PPAR-γ	Native ligand	-222.89 ±13.42	-39.14 ± 11.71	171.29 ±14.81	-21.27 ±0.74	-112.06 ±17.25
	Compound 13	-255.40 ±11.487	-50.58 ± 9.71	201.32 ±17.74	-25.25± 0.84	-129.92 ±17.38
NF-κB	Native ligand	-229.25 ± 12.56	-60.86 ± 10.08	157.56±14.77	-20.55 ± 0.77	-153.12±15.04
	Compound 13	-238.40 ±15.32	-55.39 ± 18.89	219.02±26.68	-24.32 ±1.09	-99.09 ± 17.21

The SASA profiles revealed that the compound 13 complex had a moderately higher solvent-exposed surface area compared to the native ligand, which may indicate a slightly more open conformation of the receptor–ligand interface. Meanwhile, the Rg analysis showed consistent structural compactness throughout the 100-ns trajectory, confirming that both complexes retained their globular structure during the simulation.

These molecular dynamics observations were further supported by the MM-PBSA binding energy analysis (Table 3). The total binding energy of compound 13 with PPAR-γ (-129.92 ± 17.38 kJ/mol) was lower than that of the native ligand (-112.06 ± 17.25 kJ/mol), suggesting stronger binding affinity. In contrast, for NF-κB inducing kinase interaction, compound 13 exhibited a higher total binding energy (-99.09 ± 17.21 kJ/mol) than the native ligand (-153.12 ± 15.04 kJ/mol), indicating comparatively weaker interaction strength. Although docking results of NF-κB inducing kinase with compound 13 suggested a favorable binding pose, MM-PBSA calculations revealed a weaker binding free energy relative to the native ligand. This indicates that the native ligand forms more optimal interactions, particularly in terms of solvation and electrostatic contributions, leading to higher complex stability during molecular dynamics simulations.

Overall, these results suggest that compound 13 forms a more stable and favorable complex with PPAR-γ. In contrast, its interaction with NF-κB inducing kinase, though stable, is less energetically favorable than the native ligand. Although organic selenium has been reported to influence NF-κB–associated responses, the present findings suggest that its primary mechanism involves modulation of PPAR-γ, with downstream attenuation of NF-κB activity occurring indirectly via redox-dependent signaling crosstalk [29]. This in silico study can be correlated with several in vitro and in vivo studies on the effects of selenium on PPAR-γ and NF-κB expression [9, 30]

4. Conclusion

In this study, compound 13, also known as Ebselen, demonstrated strong interactions with the target receptor PPAR-γ as indicated by its low binding free energy. RMSD and RMSF showed good stability of the compound in complex with the receptor, suggesting its primary mechanism of action. Meanwhile, NF-κB inhibition was not the primary interaction for compound 13. With these characteristics, compound 13 shows potential as a candidate for heart protection via the PPAR pathway and warrants further research for experimental validation.

Acknowledgement

We would like to thank Salsa Sagitasa, Taufik M. Fakih, and Dwi Syah F. Ramadhan for assisting with the in silico studies.

References

[1] George A. Mensah, Gregory A. Roth, Valentin Fuster, The Global Burden of Cardiovascular Diseases and Risk Factors: 2020 and Beyond, *Journal of the American College of Cardiology*, 74, 20, (2019), 2529-2532 https://doi.org/10.1016/j.jacc.2019.10.009

[2] Darryl P. Leong, Philip G. Joseph, Martin McKee, Sonia S. Anand, Koon K. Teo, Jon-David Schwalm, Salim Yusuf, Reducing the Global Burden of Cardiovascular Disease, Part 2: Prevention and Treatment of Cardiovascular Disease, *Circulation Research*, 121, 6, (2017), 695-710 https://doi.org/10.1161/CIRCRESAHA.117.311849

[3] Carina Benstoem, Andreas Goetzenich, Sandra Kraemer, Sebastian Borosch, William Manzanares, Gil Hardy, Christian Stoppe, Selenium and Its Supplementation in Cardiovascular Disease—What do We Know?, *Nutrients*, 7, 5, (2015), 3094-3118 https://doi.org/10.3390/nu7053094

[4] Ujang Tinggi, Selenium: its role as antioxidant in human health, *Environmental Health and Preventive Medicine*, 13, 2, (2008), 102-108 https://doi.org/10.1007/s12199-007-0019-4

[5] Sibel Gunes, Varol Sahinturk, Pinar Karasati, Ilknur Kulcanay Sahin, Adnan Ayhanci, Cardioprotective Effect of Selenium Against Cyclophosphamide-Induced Cardiotoxicity in Rats, *Biological Trace Element Research*, 177, 1, (2017), 107-114 https://doi.org/10.1007/s12011-016-0858-1

[6] Jie Yang, Yuan Zhang, Sattar Hamid, Jingzeng Cai, Qi Liu, Hao Li, Rihong Zhao, Hong Wang, Shiwen Xu, Ziwei Zhang, Interplay between autophagy and apoptosis in selenium deficient cardiomyocytes in chicken, *Journal of Inorganic Biochemistry*, 170, (2017), 17-25 https://doi.org/10.1016/j.jinorgbio.2017.02.006

[7] Hongmei Liu, Huibi Xu, Kaixun Huang, Selenium in the prevention of atherosclerosis and its underlying mechanisms, *Metallomics*, 9, 1, (2016), 21-37 https://doi.org/10.1039/c6mt00195e

[8] Sofia Bronzato, Alessandro Durante, Dietary Supplements and Cardiovascular Diseases, *International Journal of Preventive Medicine*, 9, 1,

(2018), 80 https://doi.org/10.4103/ijpvm.IJPVM_179_17

[9] Chang Feng, Dandan Li, Min Chen, Liping Jiang, Xiaofang Liu, Qiujuan Li, Chengyan Geng, Xiance Sun, Guang Yang, Lianchun Zhang, Xiaofeng Yao, Citreoviridin induces myocardial apoptosis through PPAR-γ-mTORC2-mediated autophagic pathway and the protective effect of thiamine and selenium, *Chemico-Biological Interactions*, 311, (2019), 108795 https://doi.org/10.1016/j.cbi.2019.108795

[10] Sascha Sauer, Ligands for the Nuclear Peroxisome Proliferator-Activated Receptor Gamma, *Trends in Pharmacological Sciences*, 36, 10, (2015), 688-704 https://doi.org/10.1016/j.tips.2015.06.010

[11] Shanky Garg, Sana Irfan Khan, Rajiv Kumar Malhotra, Manish Kumar Sharma, Manoj Kumar, Punit Kaur, Tapas Chandra Nag, RumaRay, Jagriti Bhatia, Dharamvir Singh Arya, The molecular mechanism involved in cardioprotection by the dietary flavonoid fisetin as an agonist of PPAR-γ in a murine model of myocardial infarction, *Archives of Biochemistry and Biophysics*, 694, (2020), 108572 https://doi.org/10.1016/j.abb.2020.108572

[12] Manjunatha S., Althaf Hussain Shaik, Maruthi Prasad E., Suliman Yousef Al Omar, Altaf Mohammad, Lakshmi Devi Kodidhela, Combined cardio-protective ability of syringic acid and resveratrol against isoproterenol induced cardio-toxicity in rats via attenuating NF-kB and TNF-α pathways, *Scientific Reports*, 10, 1, (2020), 3426 https://doi.org/10.1038/s41598-020-59925-0

[13] Antonella Fiordelisi, Guido Iaccarino, Carmine Morisco, Enrico Coscioni, Daniela Sorriento, NFkappaB is a Key Player in the Crosstalk between Inflammation and Cardiovascular Diseases, *International Journal of Molecular Sciences*, 20, 7, (2019), 1599 https://doi.org/10.3390/ijms20071599

[14] Simone Polvani, Mirko Tarocchi, Andrea Galli, PPARγ and Oxidative Stress: Con(β) Catenating NRF2 and FOXO, *PPAR Research*, 2012, 1, (2012), 641087 https://doi.org/10.1155/2012/641087

[15] Cristina W. Nogueira, Nilda V. Barbosa, João B. T. Rocha, Toxicology and pharmacology of synthetic organoselenium compounds: an update, *Archives of Toxicology*, 95, 4, (2021), 1179-1226 https://doi.org/10.1007/s00204-021-03003-5

[16] Ahmed Rakib, Zulkar Nain, Saad Ahmed Sami, Shafi Mahmud, Ashiqul Islam, Shahriar Ahmed, Adnan Bin Faisul Siddiqui, S M Omar Faruque Babu, Payar Hossain, Asif Shahriar, Firzan Nainu, Talha Bin Emran, Jesus Simal-Gandara, A molecular modelling approach for identifying antiviral selenium-containing heterocyclic compounds that inhibit the main protease of SARS-CoV-2: an *in silico* investigation, *Briefings in Bioinformatics*, 22, 2, (2021), 1476-1498 https://doi.org/10.1093/bib/bbab045

[17] Beena Gobind Singh, Amit Kunwar, In Silico Investigation on the Binding of Organoselenium Compounds with Target Proteins of SARS-CoV-2 Infection Cycle, *ChemRxiv*, (2020), https://doi.org/10.26434/chemrxiv.12594134.v1

[18] Ajay N. Jain, Anthony Nicholls, Recommendations for evaluation of computational methods, *Journal of Computer-Aided Molecular Design*, 22, 3, (2008), 133-139 https://doi.org/10.1007/s10822-008-9196-5

[19] David Ramírez, Julio Caballero, Is It Reliable to Take the Molecular Docking Top Scoring Position as the Best Solution without Considering Available Structural Data?, *Molecules*, 23, 5, (2018), 1038 https://doi.org/10.3390/molecules23051038

[20] Kexue Li, Lawrence R. McGee, Ben Fisher, Athena Sudom, Jinsong Liu, Steven M. Rubenstein, Mohmed K. Anwer, Timothy D. Cushing, Youngsook Shin, Merrill Ayres, Fei Lee, John Eksterowicz, Paul Faulder, Bohdan Waszkowycz, Olga Plotnikova, Ellyn Farrelly, Shou-Hua Xiao, Guoqing Chen, Zhulun Wang, Inhibiting NF-κB-inducing kinase (NIK): Discovery, structure-based design, synthesis, structure–activity relationship, and co-crystal structures, *Bioorganic & Medicinal Chemistry Letters*, 23, 5, (2013), 1238-1244 https://doi.org/10.1016/j.bmcl.2013.01.012

[21] Mark James Abraham, Teemu Murtola, Roland Schulz, Szilárd Páll, Jeremy C. Smith, Berk Hess, Erik Lindahl, GROMACS: High performance molecular simulations through multi-level parallelism from laptops to supercomputers, *SoftwareX*, 1-2, (2015), 19-25 https://doi.org/10.1016/j.softx.2015.06.001

[22] Pekka Mark, Lennart Nilsson, Structure and Dynamics of the TIP3P, SPC, and SPC/E Water Models at 298 K, *The Journal of Physical Chemistry A*, 105, 43, (2001), 9954-9960 https://doi.org/10.1021/jp003020w

[23] Ulrich Essmann, Lalith Perera, Max L. Berkowitz, Tom Darden, Hsing Lee, Lee G. Pedersen, A smooth particle mesh Ewald method, *The Journal of Chemical Physics*, 103, 19, (1995), 8577-8593 https://doi.org/10.1063/1.470117

[24] Samuel Genheden, Ulf Ryde, The MM/PBSA and MM/GBSA methods to estimate ligand-binding affinities, *Expert Opinion on Drug Discovery*, 10, 5, (2015), 449-461 https://doi.org/10.1517/17460441.2015.1032936

[25] Stephanie N. Lewis, Zulma Garcia, Raquel Hontecillas, Josep Bassaganya-Riera, David R. Bevan, Pharmacophore modeling improves virtual screening for novel peroxisome proliferator-activated receptor-gamma ligands, *Journal of Computer-Aided Molecular Design*, 29, 5, (2015), 421-439 https://doi.org/10.1007/s10822-015-9831-x

[26] Pipat Tangjaidee, Peter Swedlund, Jiqian Xiang, Hongqing Yin, Siew Young Quek, Selenium-enriched plant foods: Selenium accumulation, speciation, and health functionality, *Frontiers in Nutrition*, 9, (2023), 962312 https://doi.org/10.3389/fnut.2022.962312

[27] Gayani Nanayakkara, Thiruchelvan Kariharan, Lili Wang, Juming Zhong, Rajesh Amin, The cardio-protective signaling and mechanisms of adiponectin, *American Journal of Cardiovascular Disease*, 2, 4, (2012), 253-266

[28] Liqin Yin, Lihui Wang, Zunhan Shi, Xiaohui Ji, Longhua Liu, The Role of Peroxisome Proliferator-Activated Receptor Gamma and Atherosclerosis: Post-translational Modification and Selective Modulators, *Frontiers in Physiology*, 13, (2022), 826811 https://doi.org/10.3389/fphys.2022.826811

[29] M. Kvandová, M. Majzúnová, I. Dovinová, The Role of PPARγ in Cardiovascular Diseases, *Physiological*

Research, 65, Suppl 3, (2016), S343-S363 https://doi.org/10.33549/physiolres.933439

[30] Wei Liu, Haidong Yao, Wenchao Zhao, Yuguang Shi, Ziwei Zhang, Shiwen Xu, Selenoprotein W was Correlated with the Protective Effect of Selenium on Chicken Myocardial Cells from Oxidative Damage, *Biological Trace Element Research*, 171, 2, (2016), 419-426 https://doi.org/10.1007/s12011-015-0529-7